Wireless electrodeless piezomagnetic biosensor with an isolated nickel oscillator

Hirotsugu Ogi, Kazuma Motohisa, Takashi Matsumoto, Tomoo Mizugaki, and Masahiko Hirao

Graduate School of Engineering Science, Osaka University
Machikaneyama 1-3, Toyonaka, Osaka 560-8531, Japan

Abstract

This study presents a fundamental concept of piezomagnetic biochemical sensor driven in a wireless-electrodeless manner. A stepped cylindrical rod of nickel is used as the oscillator, which traps the vibrational energy of axially-polarized surface-shear waves in the central part, where the diameter is slightly larger. A meander-line coil surrounding the oscillator with an air gap can cause and detect the resonant vibrations of the surface-shear waves via the piezomagnetic effect. The resonant frequency of the trapped-mode resonance is continuously measured to detect human immunoglobulin G (IgG). It decreased by 0.08% when a solution containing IgG was injected into the glass cell where the oscillator was placed alone. This oscillator is useful for fundamental studies of various biochemical reactions in a closed system in different environmental gases and different pressures.

Key words: biosensor, magnetostriction, wireless, IgG, nickel, noncontacting

1 Introduction

Piezoelectric oscillators have been intensively studied for the purpose of the detection of biochemical substances. Resonant frequencies of an oscillator decrease when the target substance is adsorbed on its modified surface because of the mass loading and mechanical loss due to the viscoelastic effect of the resonating system. Quartz crystals, especially AT-cut crystals, are most widely used for their high piezoelectricity and low temperature derivatives of the elastic constants. Muramatsu *et al.* (1987) detected the change of the resonant frequency of the 9-MHz AT-cut quartz plate for quantitative evaluation of concentration of immunoglobulin G (IgG). Suri *et al.* (1994) detected immunoglobulin M with the 9-MHz AT-cut quarts. Liu *et al.* (2003a) used the 10-MHz AT-cut quartz crystal with gold electrodes for the study of the

real-time monitoring of a molecular recognition between protein and immobilized drug ligand. Halámek *et al.* (2002) used the 10-MHz AT-cut quartz for the detection of cocaine. Pan & Shih (2004) detected IgG using the 10-MHz quartz crystal with their faces coated by C_{60}-anti-human IgG. Recently, surface-shear-horizontal waves have been adopted for the liquid based sensing systems, showing higher sensitivity and faster measurements (Martin *et al.* (2004); Hur *et al.* (2005); Yamazaki *et al.* (2000)). Thus, many researchers employed piezoelectric crystals with metallic electrodes for immunosensors. Most of them, however, required wires and all of them needed electrodes. Our primary purpose in this study is to develop a wireless-electrodeless oscillator for a biochemical sensor. To our knowledge, no wireless-electrodeless biochemical sensor is reported.

There are two challenges for the development of highly sensitive and functional resonator. First is trapping of vibrational energy within an intended part of the oscillator. Acoustic resonators must be mechanically supported and if vibrational energy is significant at the points of contact, a leakage of acoustic energy into the supporting structure occurs and the Q value decreases. Second is establishment of noncontacting-electrodeless measurements. Electrodes deposited on the oscillator affects resonant frequencies, and they sometimes deteriorate resonator's sensing ability. Obviously, an electrodeless oscillator is preferable in the use at elevated temperatures. A wireless measurement enables us to measure changes in resonant frequencies in an isolated system, which contributes to understanding of fundamentals in biochemical reactions with various environment gases and various pressures.

Recently, we developed a method to generate and detect resonant vibrations of the axial-shear wave in a ferromagnetic cylindrical rod with a noncontacting manner (Ogi *et al.* (1997, 2002)), and moreover succeeded in trapping their vibrational energy in the central part of a stepped rod (Ogi *et al.* (2004)). Following these achievements, we here intend to establish the wireless-electrodeless oscillator for biochemical sensors using the piezomagnetic effect of a nickel stepped rod. This technique is applied to the detection of the human IgG captured by protein A immobilized on the surface of the cylindrical oscillator.

2 Trapped Modes of Axial-Shear Waves

Thompson (1979) revealed that surface-horizontal waves can be excited and detected on a ferromagnetic plate using a flat meander-line coil and the static magnetic field applied parallel to the straight parts of the meander-line coil. The coupling is based on the magnetostriction (piezomagnetic) response of the material. The present authors extended his measurement to cylindrical rods and analyzed the excitation and detection mechanisms (Ogi (1997); Ogi *et al.*

(2002, 2003)), and proposed a noble methodology for generation and detection of the axial-shear resonances with a noncontacting manner in a cylindrical rod (Hirao & Ogi (2003)).

The axial-shear wave is a surface shear-horizontal wave, which propagates along the circumferential direction with the polarization along the axial direction. Figure 1 shows the principle of the wireless-electrodeless acoustic coupling for axial-shear waves. A meander-line coil surrounds the cylindrical rod with an air gap and induces the dynamic fields $\mathbf{H}_\omega$ along the circumferential direction on the rod surface. A permanent magnet placed at an end of the rod applies a static magnetic field $\mathbf{H}_0$ along the axial direction. When a sinusoidal current is applied to the meander-line coil, the total field oscillates about the axial direction at the same frequency as the driving current, producing shearing vibration through the magnetostriction effect. The surface shear wave is then generated to propagate along the circumference direction with the axial polarization, that is called the axial shear wave. The meander-line coil also receives the axial-shear wave through the reverse magnetostrictive effect. An excitation with long tone bursts causes interference of the axial shear waves and a frequency scan detects the resonant peak, at which all the shear waves overlap coherently to produce large amplitude.

For a non-stepped cylindrical rod of infinite long, the frequency equation of the axial-shear-wave resonance is given by (Johnson *et al.* (1994))

$$nJ_n\left(\tilde{\eta}_n\right) - \tilde{\eta}_n J_{n+1}\left(\tilde{\eta}_n\right) = 0. \tag{1}$$

Here, n denotes the wavenumber in the circumferential direction and it equals the number of turns of the meander-line coil (Hirao & Ogi (2003)). $\tilde{\eta}_n$ denotes the wavenumber in the radial direction normalized by the radius of the rod a. The resonant frequencies ω_c are then determined by

$$\omega_c = \frac{\tilde{\eta}_n v_s}{a}, \tag{2}$$

with the shear-wave velocity v_s.

Johnson (1996) showed that there are torsional-vibration modes in a stepped cylindrical rod, whose vibrational energy is trapped in the central part of the rod where the diameter is slightly larger than those outside the steps. Following his work, we found that vibrational energy of the axial-shear-wave resonances can also be trapped in the central part of a stepped cylindrical rod with sufficiently large steps and derived the frequency equation of the trapped

modes of axial-shear-wave resonance (Ogi *et al.* (2004)):

$$\frac{ak_1}{a'|k_2|}\tan\left(\frac{l}{2a}k_1\right) = 1, \tag{3}$$

where

$$k_1 = \tilde{\eta_n}\sqrt{\frac{C_{44}}{C_{11}}\left\{\left(\frac{\omega}{\omega_c}\right)^2 - 1\right\}}, \tag{4}$$

and

$$k_2 = \tilde{\eta_n}\sqrt{\frac{C_{44}}{C_{11}}\left\{\left(\frac{\omega}{\omega_c'}\right)^2 - 1\right\}}. \tag{5}$$

Hence, a and a' ($a > a'$) are radii inside and outside the steps of the rod, respectively (see Fig. 1). k_1 and k_2 denote wavenumbers along the axial direction at the parts of radii a and a', respectively. ω are angular frequencies of the trapped resonance modes; ω_c and ω_c' are resonant frequencies for non-stepped rods with radii a and a', respectively, and they are called cutoff frequency. C_{11} and C_{44} are two independent elastic constants of the isotropic material. When $\omega_c < \omega < \omega_c'$, k_1 is a real number but k_2 is an imaginary number and the vibrational energy exponentially decays in the smaller-radius regions as the distances from the steps increase. Thus, such a resonant mode can be trapped in the central part of the rod, that is, the trapped axial-shear-wave resonant mode.

We calculated distributions of the vibrational amplitude at the surface of the trapped mode along the axial direction for various radial ratios. We found that the amplitude decreased as the distance from the center increased in the regions outside the steps and that the larger difference between a and a', the larger the decay ratio into the outside. When $(a - a')/a$=0.0368, the same value as that of the stepped rod used in the following experiment, ratios of the amplitudes at distances of 7.5 mm and 17.5 mm from the center (the step and end positions, respectively) to the amplitude at the center were 0.204 and 1.8x10^{-5}, respectively. Thus, contacts for mechanical supports at the ends of the stepped rod have little influence on the vibrations of the trapped modes when the radius difference is large enough.

There is another important advantage in the use of the shear-horizontal surface wave. It is hardly affected by the mass of the surrounding solution because of zero out-of-plane displacement.

3 MEASUREMENT

Figure 2 shows the setup for the detection of human IgG. We selected nickel as the oscillator material because of its high magnetostriction coefficients. The stepped-cylindrical nickel oscillator is placed inside a pyrex-glass tube, which is filled with phosphate buffer (0.8 ml). The radius of the oscillator at the central part (a) is 4.750 mm and those at the outside regions (a') are 4.575 mm ($\Delta a/a = 3.68\%$). Total length of the oscillator is 35 mm and length of the central part is 15 mm. Ends of the oscillator are supported by teflon fixtures. An Nd-Fe-B permanent magnet applies the static magnetic field along the axial direction to the oscillator for the magneto-acoustical coupling. The period of the meander-line coil is 1.3 mm. The total number of turns of the coil is 25.

The surface of the oscillator was modified as follows (Muramatsu *et al.* (1987)). It was electropolished in an electrolyte containing 8 % perchloric acid, 10 % 2-butoxyethanol, 70 % ethanol, and water for 5 min with 0.2 A. After rinsing with ultrapure water, the oscillator was immersed in a 5% γ-aminopropyl triethoxysilane for 24 h, rinsed with acetone, and dried in a vacuum. It was immersed in a 0.05 M glutaraldehyde solution for 3 h and abluted by 0.05-M phosphate buffer (pH 7). Protein A was then immobilized on the surface by immersing the oscillator into the phosphate-buffer solution containing 1 mg/ml Protein A for 24 h at 4 °C. (Protein A was obtained from Zymed Laboratories, Inc.) The remaining unreacted aldehyde was blocked with a 0.1 M glycine solution.

We applied tone-burst currents to the meander-line coil to generate the axial-shear waves. After the excitation, the same coil received reverberation signals via the piezomagnetic effect of nickel. A frequency scan provided resonant spectrum including a resonant peak. The sharpness of the peak (or Q value) increased by a factor 10-20 when we used the trapped mode, highly indicating successful trapping of vibrational energy. The measured resonant frequency agreed with that calculated by Eq.(3) within 0.2% with the use of handbook values for the shear modulus and mass density of nickel. The Lorentzian-function fitting procedure was used to determine the resonant frequency. We thus continuously repeated the measurement of the resonant frequency to record its change due to adsorption of human IgG.

4 Results and Discussions

The whole setup, including the sample solution to be injected, was placed in a temperature-controlled container, where the temperature was fixed to

30.0 ±0.01 °C. After the resonant frequency became stable, the solution was injected through the small hall of the top fixture by a syringe. The amount of the injected solution was 0.2 ml and the total amount of the solution inside the glass tube increases to 1.0 ml. Figure 3 shows typical result of the frequency response after an injection of phosphate-buffer solution containing 0.1 mg/ml human IgG. (The concentration of IgG in the glass tube is 0.02 mg/ml.) Human IgG (model num. CH0901) was obtained from Cortex Biochem, Inc. Figure 3 also shows its response when the phosphate-buffer solution alone was injected (denoted as background). After the injection of the phosphate-buffer solution containing IgG, the resonant frequency showed anomalous change and decreased monotonically while it was hardly affected by the injection of the phosphate-buffer solution without IgG. The anomalous change just after the injection will be caused by tentative forced convection by the injection. Thus, the piezomagnetic oscillator is capable of detecting human IgG in a wireless-electrodeless manner.

The fractional amount of the frequency decrease reaches $8\text{x}10^{-4}$ by 3000 s from the injection, which is considerably larger than those observed in previous studies using quartz crystals (Liu *et al.* (2003a,b); Pan & Shih (2004)) by one order of magnitude in spite of the lower frequency used in this study ($\sim$ 3 MHz). Reproducibility of this high sensitivity was well confirmed. The decrease of the resonant frequency is mainly attributed to two factors as given in detail by Voinova *et al.* (2002). One is an increase of the effective mass of the resonator system (Sauerbrey (1959)) and the other is mechanical losses due to viscosity between adsorbate and surrounding solution (Kanazawa and Gordon (1985)). These contributions are sometimes separately discussed. Quantitative evaluation of the viscoelastic effect is however not straightforward because the viscosity coefficient is usually unknown and it is highly dependent on the structure of the adsorbate, temperature, and the flow rate. Thus, we here intend to identify the dominant contribution by estimating the contribution of the mass-loading effect. Assuming the ideal case that full-length IgG molecules are densely and closely attached on the modified surface, the frequency decrease is expected to be less than $1.0\text{x}10^{-6}$. (We assumed that the height, width, and length of IgG was 9, 15, and 5 nm, respectively; and its molecular mass was 150,000 following Nollb *et al.* (1982); Sarma *et al.* (1971).) This value is much smaller than the amount of the actual frequency change. Thus, the viscoelastic mechanism should mainly contribute to the frequency decrease. Our future work includes simultaneous monitoring of frequency and internal friction during various biochemical reactions as well as improvement of the Sauerbrey equation.

5 CONCLUSIONS

The piezomagnetic cylindrical oscillator was developed for the use in the biochemical sensor. It can be activated with the wireless-electrodeless manner by the surrounding meander-line coil. The oscillator had larger diameter at the central region; the surface-shear waves can be trapped there causing little leakage of the vibrational energy into the ends, at which the rod was mechanically supported. Protein A was immobilized on the oscillator surface for the detection of human IgG. The oscillator was placed alone in a glass tube, and the resonant frequency was monitored after the injection of solution containing human IgG. The frequency decreased by 0.08%, which is larger in magnitude than those observed in previous studies with QCMs. Thus, this piezomagnetic oscillator provides a fundamental concept of a wireless-electrodeless biochemical sensor.

References

Halámek, J., Makower, A., Skládal, P. & Scheller, F. (2002). Highly sensitive detection of cocaine using a piezoelectric immunosensor. Biosensors & Bioelectronics **17**, 1045-1050.

Hur, Y., Han, J., Seon, J., Pak, Y. E., & Roh, Y. (2005). Development of an SH-SAW sensor for the detection of DNA hybridization. Sensors & Actuators A **120**, 462-467.

Hirao, M. & Ogi, H. (2003). EMATs for science and industry: Noncontact ultrasonic measurements. (Kluwer-Academic publishers, Boston).

Johnson, W., Auld, B. A., & Alers, G. A. (1994) Application of resonant modes of cylinders to case depth measurement. Rev. of Progress in QNDE, Vol.13 (Academic Press, New York) 1603-1610.

Johnson, W. (1996), Trapped torsional modes in solid cylinders. J. Acoust. Soc. Am. **100**, 285-293.

Kanazawa, K.K., & Gordon, J.G., (1985). The oscillation frequency of a quartz resonator in contact with a liquid. Anal. Chim. Acta **175**, 99-105.

LiuCY., Yu, X., Zhao, R., Shangguan, D., Bo, Z. & Liu, G. (2003a). Real time kinetic analysis of the interaction between immunoglobulin G and histidine using quartz crystal microbalance biosensor in solution. Biosensors & Bioelectronics **18**, 1419-14279.

LiuCY., Yu, X., Zhao, R., Shangguan, D., Bo, Z. & Liu, G. (2003b). Quartz crystal biosensor for real-time monitoring of molecular recognition between protein and small molecular medicinal agents. Biosensors & Bioelectronics **19**, 9-19.

Martin, F., Newton, M. I., McHale, G., Melzak, K. A., & Gizeli, E. (2004). Pulse mode shear horizontal-surface acoustic wave (SH-SAW) system for liquid based sensing applications. Biosensors & Bioelectronics **19**, 627-632.

Muramatsu, H., Dicks, M. D., Tamiya, E. & Karube, I. (1987). Piezoelectric crystal Biosensor modified with protein A for Determination of immunoglobulins. Anal. Chem.. **59**, 2760-2763.

Nollb, F, Lutscha, G & Bielkab, H (1982). Structure of IgG and IgY molecules in ribosome?Antibody complexes as studied by electron microscopy. Immunology Lett. **4**, 117-123.

Ogi, H. (1997). Field dependence of coupling efficiency between electromagnetic field and ultrasonic bulk waves. J. Appl. Phys. **82**, 3940-3949.

Ogi, H., Hirao, M. & Minoura, K. (1997). Noncontact Measurement of Ultrasonic Attenuation during Rotating Fatigue Test of Steel. J. Appl. Phys. **81**, 3677-3684.

Ogi, H., Minami, Y. & Hirao, M. (2002). Acoustic study of dislocation rearrangement at later stages of fatigue: Non-contact prediction of remaining life. J. Appl. Phys. **90**, 438-442.

Ogi, H., Goda, E. & Hirao, M. (2003) Increase of efficiency of magnetostriction SH-wave EMAT by angled bias field: Piezomagnetic theory and measurement. Jpn. J. Appl. Phys., **42**, 3020-3024.

Ogi, H., Wada, K. & Hirao, M. (2004). Energy trap for axial-shear-wave resonance in a stepped cylindrical rod: theory and measurement. Jpn. J. Appl. Phys. **43**, 3024-3026.

Pan, N. Y. & Shih, J. S. (2004). Piezoelectric crystal immunosensors based on immobilized fullerene C60-antibodies. Sensors & Actuators B **98**, 180-187.

Sauerbrey, G (1959). The use of quartz oscillators for weighing thin layers and for microweighing. Z. Phys. **155**, 206-222.

Sarma, V., Silverton, E., Davies, D. & Terry, W. (1971). The three-dimensional structure at 6 A resolution of a Human γG1 immunoglobulin molecule. J. Biol. Chem. **246**, 3753-3759.

Suri, C. R., Raje, M. & Mishra, G. C. (1994). Determination of immunoglobulin M concentration by piezoelectric crystal immunobiosensor coated with protamine. Biosensors & Bioelectronics **9**, 535-542.

Thompson, R. B. (1979). Generation of horizontally polarized shear-waves in ferromagnetic materials using magnetostrictively coupled meander-coil electromagnetic transducers. Appl. Phys. Lett. **34**, 175-177.

Voinova, M. V., Jonson, M. & Kasemo, B. (2002). eMissing mass' effect in biosensor's QCM applications. Biosensors & Bioelectronics **17**, 835-841.

Yamazaki, T., Kondoh, J., Matsui Y., & Shiokawa, S. (2000). Estimation of components and concentration in mixture solutions of electrolytes using a liquid flow system with SH-SAW sensor. Sensors & Actuators A **83**, 34-39.

Figure Caption

Fig. 1 (a)Generation and detection of the axial-shear-wave resonances by the meander-line coil surrounding the stepped cylindrical rod. (b)Schematic of the generation mechanism of the axial-shear wave by the piezomagnetic effect.

Fig. 2 Setup of the wireless-electrodeless detection of human IgG. Left part of the figure shows the cross-section of the system. The oscillator is located in the pyrex-glass tube filled with the phosphate buffer. The meander-line coil with $n = 25$ is placed on the outer surface of the glass tube. The nickel oscillator is isolated from the wire and electrodes.

Fig. 3 Fractional change of the resonant frequencyof the trapped axial-shear-wave mode of the nickel oscillator after the injection of the solution containing IgG. Response after an injection of the phosphate buffer without IgG is also shown (background).

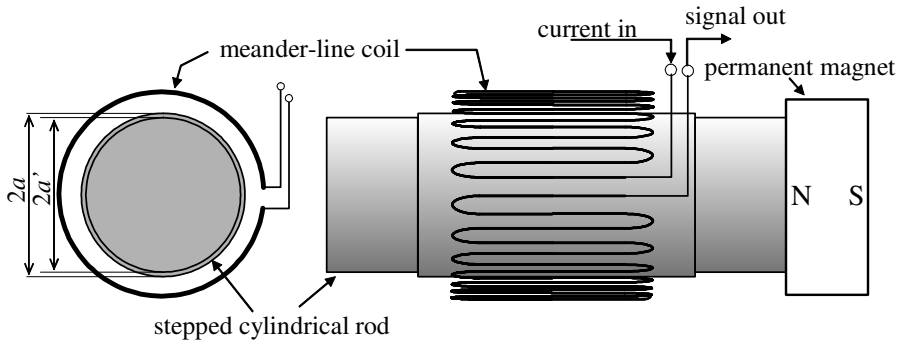

(a) stepped oscillator and meander-line coil

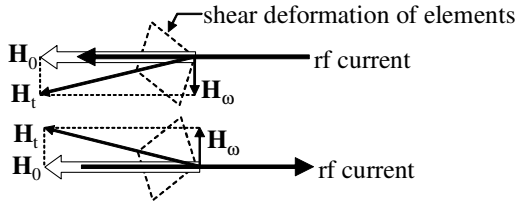

(b) periodic shear deformation caused by magnetostriction

Fig. 1.

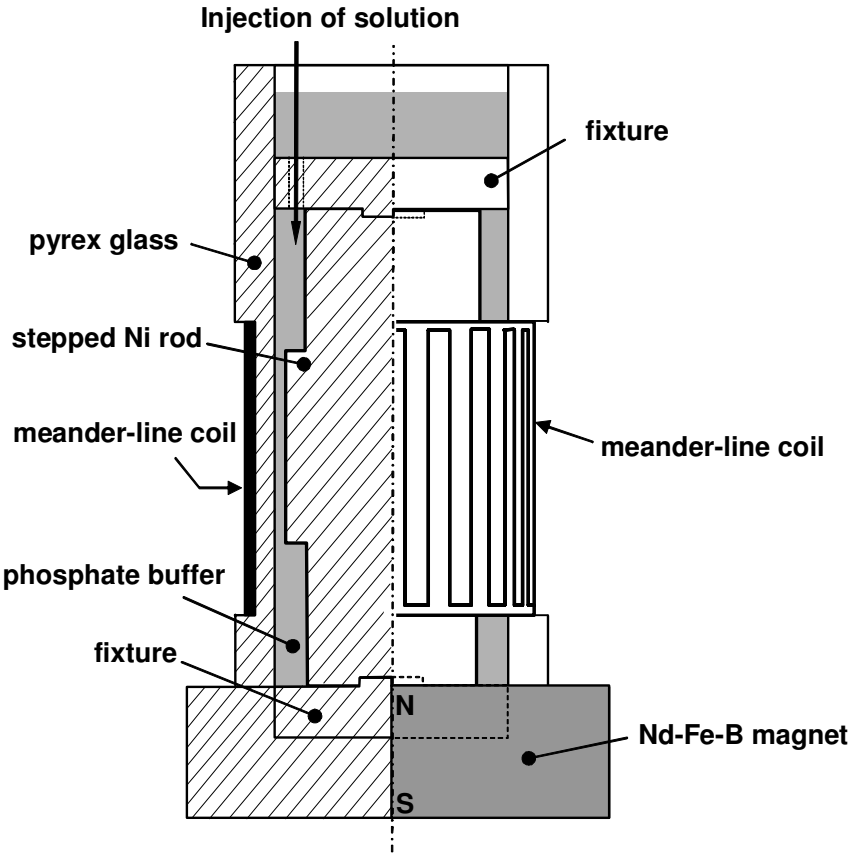
Injection of solution
fixture
pyrex glass
stepped Ni rod
meander-line coil
meander-line coil
phosphate buffer
fixture
N
Nd-Fe-B magnet
S

Fig. 2.

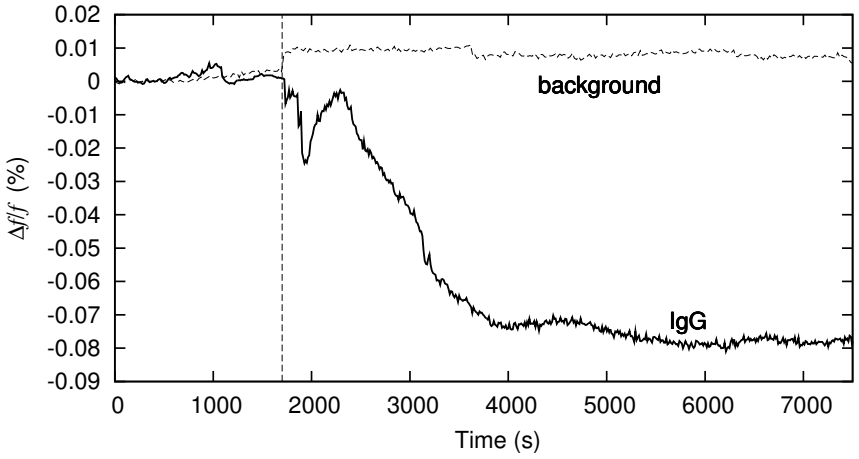
0.02
0.01
0
-0.01
-0.02
-0.03
-0.04
-0.05
-0.06
-0.07
-0.08
-0.09
Δf/f (%)
0
1000
2000
3000
4000
5000
6000
7000
Time (s)
background
IgG

Fig. 3.